Hindawi Publishing Corporation
International Journal of Rotating Machinery
Volume 2007, Article ID 90631, 8 pages
doi:10.1155/2007/90631

Research Article

Analysis of Rotor-to-Stator Rub in a Large Steam Turbogenerator

Paolo Pennacchi and Andrea Vania

Dipartimento di Meccanica, Politecnico di Milano, 20156 Milan, Italy

Received 6 June 2006; Accepted 19 December 2006

Recommended by K. Kawaike

Rotor-to-stator rub is a very common topic in rotor dynamics and several models have been proposed in the literature. Anyhow these models are often able to explain only the experimental dynamical behaviour of simple test rigs, which are deliberately reproducing a Jeffcott rotor. On the contrary case, histories related to real machines are seldom presented and analysed. The aim of this paper is to present an actual case history of a large turbogenerator unit that was subjected to partial arc rubs. The experimental results are shown and discussed along with the model-based diagnostic strategy employed to identify the fault severity and the location of the shaft cross-sections where the heaviest rubs occurred. Comparisons between experimental data and simulated vibrations caused by the identified fault are shown to validate the proposed methodology.

1. INTRODUCTION

The study of the rotor-to-stator rub phenomenon is one of the most relevant topics in rotor dynamics, due to the fact that actual rotating machines operate on a working fluid, thus many parts of small clearances are present between the rotor and its casing. Many different theoretical models have been developed in the past, the majority of them are addressed to give a qualitative explanation of the rub, using a very simplified model of the rotor and focusing their attention to the contact aspects. A comprehensive survey is given by Muszyńska [1], but research activities are still in progress as results from the recent papers (Ehehalt et al. [2]). In several cases, also experimental results related to test-rigs that are deliberately designed to reproduce Jeffcott rotors are reported; see for instance Muszyńska [1], Ehehalt et al. [2], Yamamoto, and Ishida [3].

On the contrary, few studies have been presented about the effects on large rotating machinery and this paper is intended to add a contribution in this case, presenting the analysis of case history related to a large steam turbo generator.

Radial and angular misalignments of the rotor-trains as well as high shaft vibrations induced by several machine malfunctions can cause rotor-to-stator rubs in rotormachinery. Heavy rubs can cause impacts, chaotic motions as well as sub-synchronous and super-synchronous vibrations of the shafts. On the contrary, light partial arc rubs and full-annular rubs often cause major progressive changes in the synchronous vibrations (1X). Sometimes, depending on the mechanical and thermal characteristics of the system, as well as on the shaft rotating speed, stable or unstable synchronous spiral vibrations can occur (Liebich and Gasch [4], Kellenberger [5], Bachschmid et al. [6]). In fact, the heat introduced into the shaft by the friction forces generated by the rotor-to-stator contacts induces a time-varying thermal bow of the shaft that, in consequence, causes synchronous vibrations.

Sometimes the rub phenomena that occur in operating conditions can be extinguished by changing some suitable process parameters. However, also changes in the shape and wideness of the shaft orbits as well as consequent changes in the shaft centreline position inside bearings and seals can allow the available radial clearance to become sufficient to extinguish the rubs. In this case, the end of rotor-to-stator contacts and friction forces nullifies the heat introduced in the shaft. Conversely, when rotor-to-stator rubs occur during runups and coastdowns, the shaft bow evolution can become more complex owing to the passing through shaft flexural critical speeds as well as to the changes in rotating speed and unbalance forces.

The equivalent bending moments that cause the shaft bow induced by the rubs can be estimated by means of model-based identification methods developed in the frequency domain (Bachschmid et al. [7]). These techniques minimise the error between the machine experimental vibrations and the response obtained using the model of the fully assembled machine. In the past, the authors developed model-based diagnostic techniques aimed to identify type, severity, and location of faults in rotating machines as well as methods aimed to measure the accuracy of the results provided by the identification process (Vania and Pennacchi [8]).

In this paper, the results obtained by applying these methods to the analysis of the experimental response of a power unit that was subjected to large partial arc rubs are shown and discussed together with the strategy used to identify the fault severity and the location of the cross-sections where the heaviest rubs occurred.

The bending moments associated with the shaft bow caused by the rubs can be evaluated by means of more complex and accurate model-based methods in which the motion and thermal equations of the fully assembled machine are combined each other and are integrated in the time domain (Bachschmid et al. [6]). These methods allow the time history of the rubs to be studied and simulated. In general, these techniques require the equivalent parameters of some machine thermal properties to be estimated. The accuracy of the results provided by these methods can be significantly affected by the care with which the model has been tuned. Therefore, the rate of the increase of the magnitude of the time dependent bending moments induced by the rubs, estimated by means of the approximated methods developed in the frequency domain described in this paper, can give very helpful information about some thermal and mechanical properties of the system. This diagnostic approach can be considered as a preliminary analysis of rub phenomena the results of which can improve the adequacy of the model used by more complex and accurate methods developed in the time domain.

2. FAULT IDENTIFICATION STRATEGY

Some model-based methods aimed to identify faults in rotating machines are developed in the time domain (Platz and Markert [9]); however, the approach described in this paper, as well as many fault identification techniques, has been developed in the frequency domain. The model-based technique used in this investigation to identify machine faults is described in detail by Bachschmid et al. [7] and Pennacchi et al. [10]. This method enables simultaneous faults to be identified. An outline of this identification technique is shown below for the case of a single fault only.

As said above, the dynamic effects of machine faults can be simulated by means of suitable sets of forces and moments that are applied to nodes of the finite element (FE) model of the machine rotor train. By assuming that the system is linear and time invariant, the following equation can be written for each harmonic component, of order n, of the machine excitations:

$$\left[-(n\Omega)^2\mathbf{M} + i\,n\Omega(\mathbf{D}+\Omega\mathbf{G}) + \mathbf{K}\right]\mathbf{X}_n = \mathbf{F}_n(n\Omega), \tag{1}$$

where Ω is the machine rotating speed, $\mathbf{K}$, $\mathbf{M}$, and $\mathbf{D}$ are the stiffness, mass, and damping matrices of the fully assembled system composed of rotor-train, journal bearings, and foundation structure, while $\mathbf{G}$ is the gyroscopic matrix of the shaft train. The terms of the force vector $\mathbf{F}_n$ are the equivalent excitations used to model the fault that must be identified. The terms of vector $\mathbf{F}_n$ depend on the excitation frequency $n\Omega$. The quantity in the square brackets of (1) is the mechanical impedance matrix of the system. The harmonic content of the excitations, as well as the number of not-null terms of vector $\mathbf{F}_n$, depends on the type of the fault. A large review about fault modelling by means of equivalent force systems is illustrated by Bachschmid et al. [7] along with some model validations. Although (1) can be written for every rotating speed of a transient, only the experimental vibration data collected for a limited number of suitable rotating speeds are analysed in order to avoid an overabundance of nearly identical observations that could cause numerical problems or identification errors. Moreover, the analysis of an excessive amount of experimental data could cause the solution of the problem to become time consuming without causing a significant increase of the result accuracy. Equation (1) can be solved to obtain the machine vibrations, by defining the transfer matrix $\mathbf{H}_n$ as the inverse of the mechanical impedance matrix:

$$\mathbf{X}_n = \left[-(n\Omega)^2\mathbf{M} + i\,n\Omega(\mathbf{D}+\Omega\mathbf{G}) + \mathbf{K}\right]^{-1}\mathbf{F}_n(n\Omega), \tag{2}$$

that is,

$$\mathbf{X}_n = \mathbf{H}_n\mathbf{F}_n(n\Omega). \tag{3}$$

Usually, the absolute vibrations of the shafts are measured in correspondence of a limited number of cross-sections that often coincide with the machine supports. Therefore, a vector $\mathbf{X}_m$, the terms of which are the shaft displacements associated with the degrees of freedom (DOF) along which the machine vibrations are measured, must be defined. A unique set of (2) can be written considering different rotating speed values. Then, the rows in (2) are rearranged, by partitioning the transfer matrix $\mathbf{H}_n$, in order to split the vector $\mathbf{X}_m$, from the vector $\mathbf{X}_r$, the terms of which are the displacements evaluated at the remaining DOFs of the rotor system model. Therefore, (2) can be rewritten in the following form, in which any dependence on both Ω and harmonic order n has been omitted for the sake of brevity:

$$\begin{aligned}\mathbf{X}_m &= \mathbf{H}_m\mathbf{F}_n,\\ \mathbf{X}_r &= \mathbf{H}_r\mathbf{F}_n.\end{aligned} \tag{4}$$

Considering only the first set of (4) and the vector $\mathbf{X}_{\text{ex}}$, the terms of which are the experimental transient vibrations that correspond to the terms of the vector $\mathbf{X}_m$, it is possible to determine the error, $\boldsymbol{\delta}$, between simulated vibrations and experimental data,

$$\delta = \mathbf{X}_m - \mathbf{X}_{\text{ex}} = \mathbf{H}_m\mathbf{F}_n - \mathbf{X}_{\text{ex}}. \tag{5}$$

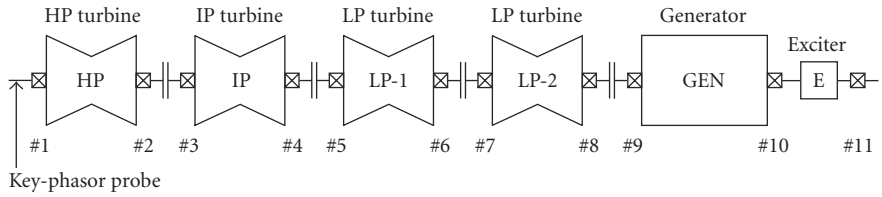

Figure 1: Machine train diagram.

Then, the equivalent excitations $\mathbf{F}_n$ can be estimated by weighted least squares error methods. In order to allow easier comparisons between the errors obtained with the identification of different faults a relative error, ε, can be evaluated using the following expression:

$$\varepsilon = \left(\frac{[\mathbf{X}_m - \mathbf{X}_{\text{ex}}]^{*T} [\mathbf{X}_m - \mathbf{X}_{\text{ex}}]}{\mathbf{X}_{\text{ex}}^{*T} \mathbf{X}_{\text{ex}}} \right). \tag{6}$$

Usually, the scalar error ε is called residual. The location of the excitations $\mathbf{F}_n$ used to model single or multiple faults must be changed along the rotor span to identify the actual location of the fault. Therefore, many estimates of the residual ε are provided by a fault identification process and more than one type of fault could be modelled accordingly with the fault symptoms pointed out by the monitoring data. The most probable fault is associated with the minimum residual. This strategy allows the type, the severity, and the location of the fault to be identified.

3. CASE HISTORY

The analysis of the vibrations of a 320-MW power unit allowed the capabilities of the proposed model-based diagnostic method to be validated. The machine-train was composed of a high-pressure steam turbine (HP), an intermediate-pressure turbine (IP), two low-pressure turbines (LP1, LP2) and a generator. Figure 1 shows the machine train configuration and the numbers of the eleven oil-film journal bearings that supported the shaft-train. The operating speed of the unit was 3000 rpm. Velocimeters mounted in the vertical direction near some journal bearings measured the absolute vibrations of the shafts. A proximity probe mounted in the portion of the HP turbine shaft towards the uncoupled end, before bearing no. 1 (Figure 1), was used as tachometer and keyphasor probe as well as an additional vibration measurement point.

3.1. Experimental results

The vibrations measured during normal runups and coast-downs showed that the first flexural critical speed of the HP turbine was close to 1800 rpm as shown in Figure 2.

Figures 3 and 4 show the Bode plots of the 1X vibrations measured at bearings no. 1 and no. 2 during the first start-up of the unit occurred at the end of a large planned maintenance during which the machine-train was subjected to important overhauls. When the rotating speed reached 1720 rpm, the amplitude of the HP turbine vibrations increased owing to the effects caused by the first balance resonance. However, in a very short time the vibration levels reached abnormal values.

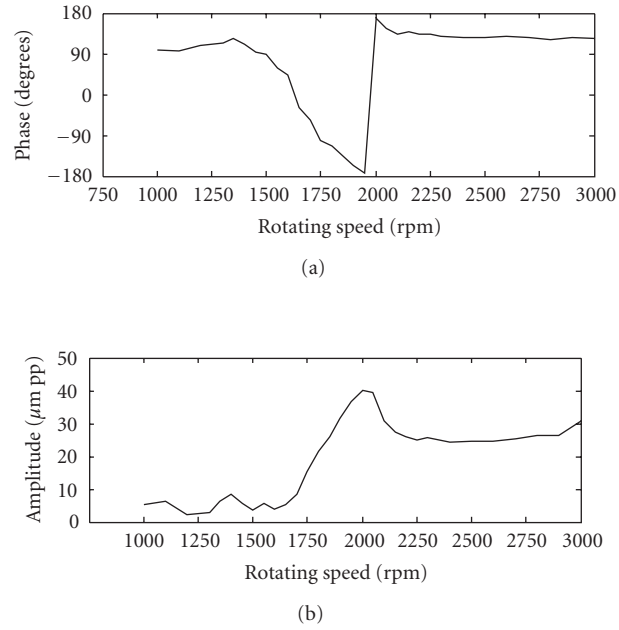

Figure 2: Bode plot of the 1X transient vibrations measured at bearing no. 2 during a normal runup.

Table 1: Amplitude of the first three harmonic orders of the shaft vibrations measured on the bearings #1 and #2 at 1720 rpm during the first aborted startup.

	Vibration amplitude		
	Harmonic orders		
	1X	2X	3X
Bearing	μm pp	μm pp	μm pp
No. 1	217	164	51
No. 2	115	33	27

At the same time, the amplitude of the 2X revolution (2X) and 3X revolution (3X) vibrations showed a quick and noticeable increase. Table 1 shows the amplitude of the 1X, 2X, and 3X vibrations measured at 1720 rpm on the bearings no. 1 and no. 2.

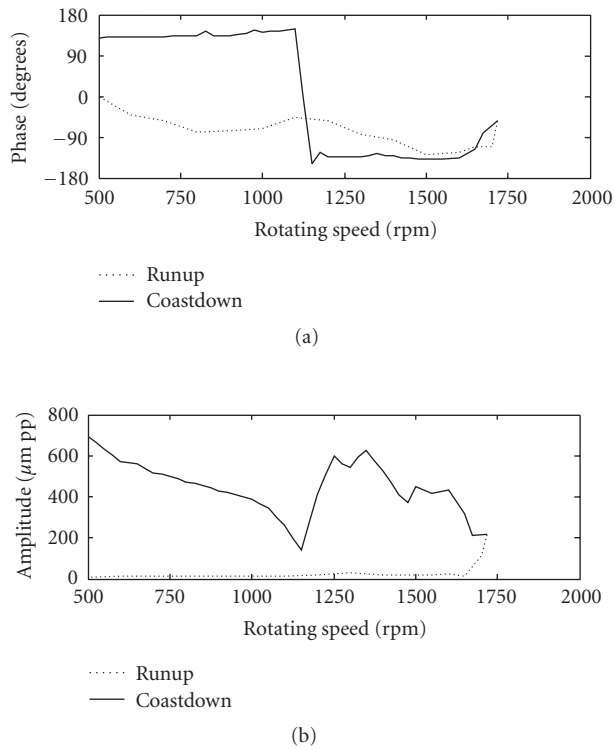

Figure 3: Bode plot of the 1X vibrations measured at bearing no. 1 during the first startup and the subsequent coastdown carried out after the rub occurrence.

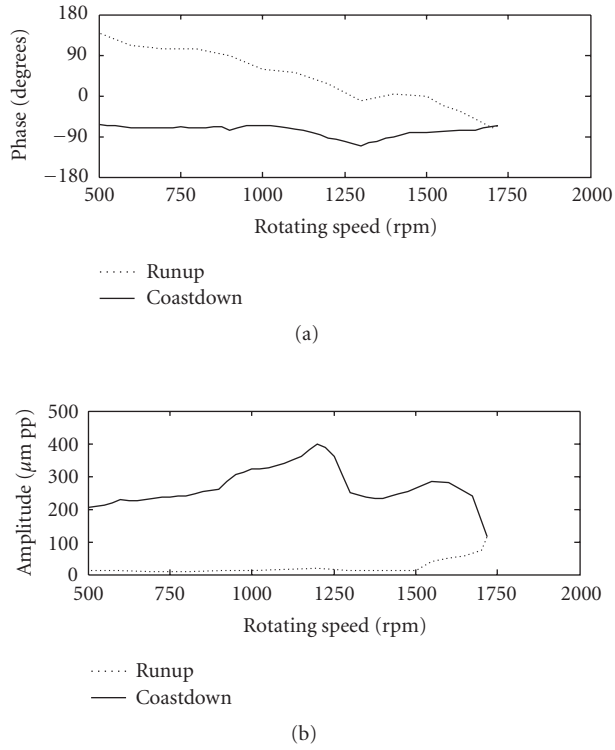

Figure 4: Bode plot of the 1X vibrations measured at bearing no. 2 during the first startup and the subsequent coastdown carried out after the rub occurrence.

Since the shaft vibrations showed clear symptoms of a machine fault, the runup was immediately aborted. The levels of the vibrations measured at bearings no. 1 and no. 2 significantly increased and in the final part of this coastdown they exceeded 700 μm pp (Figure 3) and 200 μm pp (Figure 4), respectively.

On some measurement points, the phase values of the 1X vibrations were rather different from those measured at the same rotating speed during the previous start-up. At the end of the planned maintenance, the machine-train was reassembled and aligned. However, after a final inspection the alignment of the support no. 1 was modified. The bearing casings and the pedestals were separated from the casing of the HP turbine. Therefore, in order to obtain a correct alignment between the shaft and the seals also the alignment of the HP turbine casing had to be modified. Unfortunately, this maintenance action was never done before the first start-up. Owing to this it is possible to suppose that in some cross-sections of the shaft-train, the available radial clearance between the seals and the shaft was rather small. During the first run-up, when the rotating speed approached the first balance resonance even a small amplification of the vibration levels caused rotor-to-stator rubs. Owing to the flexibility of the seal mountings it is possible to suppose that the rotor-to-seal contacts were more similar to heavy partial arc rubs, or full-annular rubs, rather than to severe impacts. The friction forces generated during these heavy contacts caused the generation of a considerable heat. Sometimes, depending on the characteristics of the rub phenomena, this heat is transmitted to the rotor through a small portion of the circumferential surface. This causes a shaft thermal bow as well as changes in the synchronous vibrations.

The effects of the rubs mainly affected the vibrations of the HP turbine, especially in the shaft portion towards the uncoupled end. It was possible to suppose that the heaviest rubs occurred in this area of the shaft train. A visual inspection confirmed this assumption.

Figure 5 shows a short windowed time record of the vibration signal provided by the keyphasor probe at the beginning of the machine trip, when the rotating speed was 1660 rpm. The height of the spike due to the passing of the shaft notch in front of the probe was much higher than the overall amplitude of the shaft vibrations. This confirms that at the beginning of the coastdown the dynamic effects caused by the rotor-to-seal rubs were evident but not yet detrimental. Figures 6 and 7 show the short time records of the vibration signal provided by the keyphasor probe during the coastdown at 1490 rpm and 160 rpm, respectively. The order analysis of the keyphasor signals illustrated in Figures 5–7 was carried out after having removed the effects of the 1X pulses.

The amplitude of the synchronous harmonic component is shown in Table 2 together with the ratio between the amplitude of the 2X and 1X vibrations. In the end, in the same table, the ratio between the amplitude of the 3X and 1X harmonic components is shown.

Figure 7 shows that in a very short time after the first occurrences of the rotor-to-seal rubs the vibrations of the HP

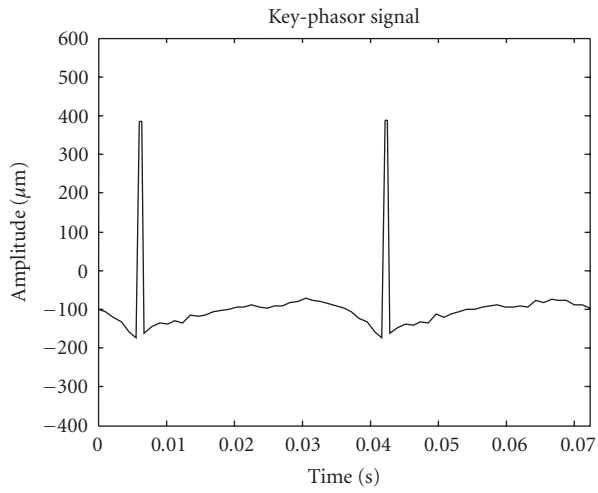

Figure 5: Time history of the lateral vibrations measured by the key-phasor probe at the beginning of the rub phenomena. Rotating speed: 1660 rpm.

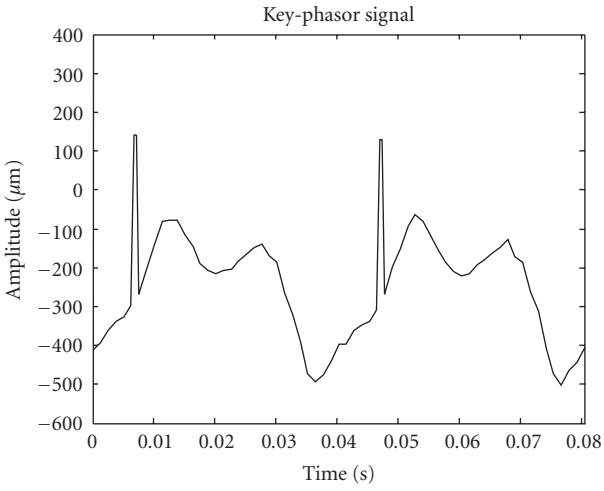

Figure 6: Time history of the lateral vibrations measured by the key-phasor probe during the coastdown carried out after the rub occurrence. Rotating speed: 1490 rpm.

turbine exhibited very high 2X and 3X harmonic components.

At the end of the coast-down, the highest contribution to the HP turbine vibrations was due to the synchronous harmonic component the amplitude of which significantly increased during the slow down while the levels of the super-synchronous components decreased (Table 2). On the basis of these experimental findings, it is possible to suppose that in the final part of the coast-down single partial arc rubs per revolution occurred in one or more cross-sections.

4. IDENTIFICATION OF THE RUB POSITION

An accurate study of the vibrations caused by rubs in rotating machines would require to simulate the thermal phe-

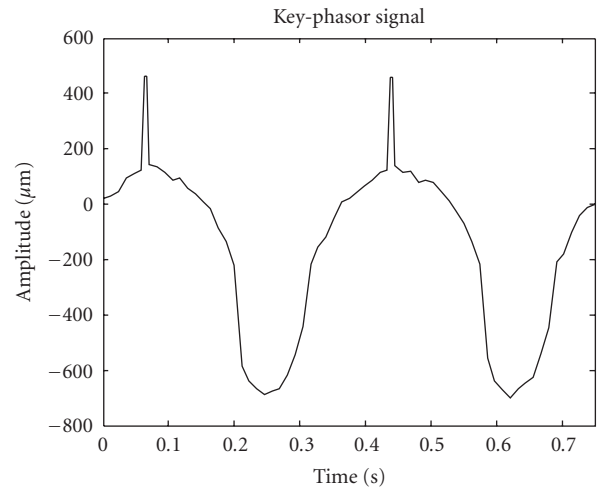

Figure 7: Time history of the lateral vibrations measured by the key-phasor probe at the end of the coastdown carried out after the rub occurrence. Rotating speed: 160 rpm.

Table 2: Harmonic content of the key-phasor signal measured during the coastdown: effects of the rub evolution.

	Rotating speed		
	1660 rpm	1490 rpm	160 rpm
1X Amplitude μm pp	65.5	298.6	771.9
Ratio: 2X/1X	0.4556	0.5063	0.3556
Ratio: 3X/1X	0.1585	0.3141	0.1252
Ratio: 4X/1X	0.1313	0.1320	0.0571

nomena induced by the friction forces. To this purpose accurate mathematical methods can be used (Liebich and Gasch [4], Kellenberger [5], Bachschmid et al. [6]). In general these methods combines thermal equations and motion equations of the system. The global set of equations must be integrated in the time domain in order to simulate the time history of machine vibrations and the rotor-to-stator contacts as well as to evaluate the shaft heating. Unfortunately, some parameters of the machine model used by these techniques are not easy to be determined with a good accuracy. This can significantly affects the reliability of the results although some main characteristics of rotor-to-stator contacts and shaft vibrations can be satisfactorily simulated.

Anyhow, the rub phenomena in rotating machines can be successfully investigated also with approximated methods developed in the frequency domain which avoid to study the thermal phenomena. In fact, these techniques consider only the equivalent dynamic effects caused by the shaft bows induced by friction forces and rotor heating. This approach cannot simulate all the physic phenomena that affect a rotating machine when rubs occur; nevertheless, it is very helpful for preliminary investigations the results of which can provide interesting information that can be used to tune more accurate methods developed in the time domain (Bachschmid et al. [6]).

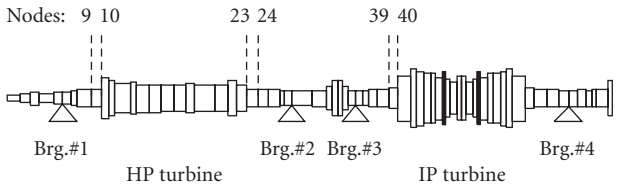

Figure 8: Finite element model of the HP turbine and IP turbine.

A model of the fully assembled machine has been developed. Figure 8 shows the FEM of the portion of the machine train composed of either HP or IP turbines.

The fault identification method described above requires to analyse the machine vibrations caused only by the faults that must be identified. In this case, the dynamic effects caused by the shaft bow induced by the rubs have been estimated by subtracting the 1X vibration vectors measured during the first aborted start-up, before the rub occurrences, from the corresponding 1X vectors measured during the coastdown occurred after the machine trip. These transient vibration data have been denoted additional vibrations. This approach is not rigorous since the rubs caused some nonlinear effects in the machine dynamic behaviour; nevertheless, the use of a linear model to study the machine response and the analysis of the additional vibrations defined by neglecting the nonlinear effects in the experimental vibrations provided satisfactory results.

The fault identification method required to define a suitable set of equivalent excitations which were able to cause 1X vibrations similar to those induced by the shaft bow generated by the rotor-to-seal rubs. It was supposed that the heaviest rubs occurred on limited portions of the rotor-train where some important seals were located. Owing to this, it was possible to suppose that the shafts were affected by one or more local bows the amplitude of which was time dependent.

Since the heaviest rubs occurred during the coast-down, the relationship between the shaft bow and the time was transformed into a relationship with the shaft rotating speed.

A shaft local bow can be simulated by applying a pair of opposite bending moments to a limited portion of the FEM of the shaft train. These moments are represented by means of synchronous rotating vectors.

In the case study described in the present paper, pairs of opposite bending moments have been applied to the ending nodes of three different beam finite elements of the shaft train model. Figure 8 shows the location of these three beam elements over the model. The number of the nodes to which these equivalent excitations have been applied is reported in Table 3.

The two pairs of opposite bending moments $\pm\mathbf{M}_1$ and $\pm\mathbf{M}_2$ have been applied at the opposite ends of the main body of the HP turbine while the pair of bending moments $\pm\mathbf{M}_3$ have been applied at the end of the main body of the IP turbine, towards the HP turbine.

Table 3: Position of the equivalent bending moments.

Bending moment	Node no.	Bending moment	Node no.
$+\mathbf{M}_1$	9	$-\mathbf{M}_1$	10
$+\mathbf{M}_2$	23	$-\mathbf{M}_2$	24
$+\mathbf{M}_3$	39	$-\mathbf{M}_3$	40

Table 4: Residuals provided by the fault identification method.

	Bearings			
	No. 1	No. 2	No. 3	No. 4
ε_i	0.1071	0.0773	0.2654	1.0580

The magnitude and the phase of each pair of bending moments were estimated by the identification method above described. The identification process was carried out considering the 1X additional vibrations measured at bearings from no. 1 to no. 4. Since the local shaft bows changed during the coast-down the corresponding bending moments have been estimated by multiple identification processes carried out at different rotating speeds.

The global residual evaluated by applying (6) to the vibration data collected at all the selected measurement points was rather small ($\varepsilon_g = 0.1166$). In addition to this, a set of partial residuals, ε_i, have been evaluated by considering the errors of the identification process associated with the ith measurement point (Table 4). All the residuals have been evaluated over the entire rotating speed range from 500 rpm to 1700 rpm.

As said above, the shaft bow induced by the rubs changed during the coastdown. Therefore, also the equivalent excitations used to simulate the dynamic effects caused by the fault depended on the rotating speed as well as on the time. Figure 9 shows the changes in magnitude and phase of the bending moments $\pm\mathbf{M}_1$, $\pm\mathbf{M}_2$, and $\pm\mathbf{M}_3$ identified over the rotating speed range from 1600 rpm to 500 rpm.

These results confirm that the heaviest rubs occurred in the area of the HP turbine towards the uncoupled end.

In the rotating speed range below 1150 rpm, the severity of the local shaft bow occurred in this portion of the shaft continuously grew during the machine slow down while the angular position of the single local bows remained nearly constant since the phases of each pair of bending moments showed only small changes in the above-mentioned range of the rotating speed. These results confirm that the heat generated by the friction forces during the rotor-to-seal contacts was introduced into the shaft, in different spaced cross-sections, over a limited portion of the circumferential surface the angular position of which was affected by small changes during the coastdown. This behaviour is not unusual when large partial arc rubs or full annular rubs occur.

The identified bending moments were used in the machine model as equivalent excitations to estimate the response caused by the rubs. In Figure 10, the 1X additional

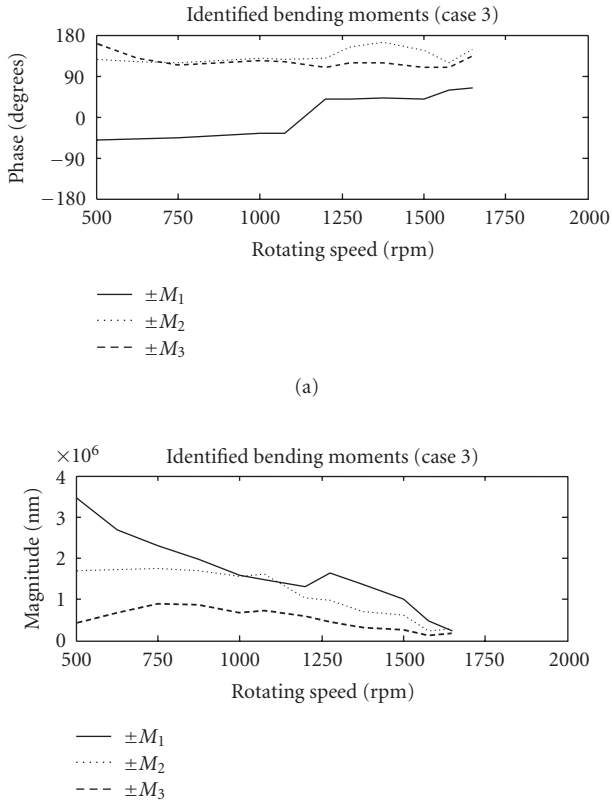

FIGURE 9: Magnitude and phase curves of the identified bending moments $\pm\mathbf{M}_1$, $\pm\mathbf{M}_2$, $\pm\mathbf{M}_3$ evaluated in the rotating speed range from 500 rpm to 1600 rpm.

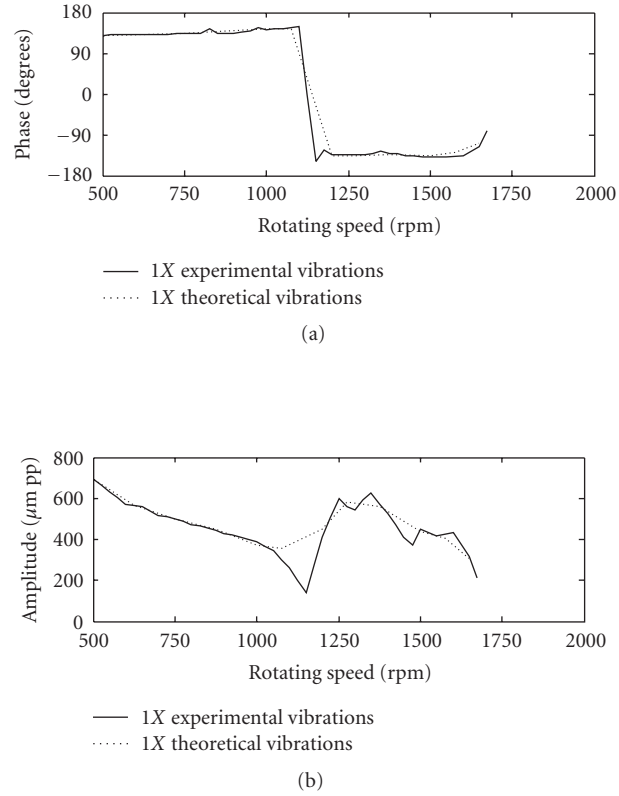

FIGURE 10: Bode plot of the 1X vibrations caused by the rubs during the coastdown. Comparison between the 1X additional vibrations measured at bearing no. 1 and the numerical results obtained using the identified bending moments.

vibrations measured at bearing no. 1 during the coastdown are compared with the respective theoretical vibrations provided by the model.

The accordance between experimental data and numerical results is rather good.

The visual inspection of the machine train carried out after this aborted start-up confirmed the occurrence of heavy rubs that caused serious damages of the journal bearings no. 1 and no. 2 as well as a noticeable wear of many seals of the HP and IP turbines. The major damages caused by the rubs were found in the HP turbine while the IP turbine was affected by minor but not negligible damages.

5. CONCLUSION

In general, the friction forces generated by partial arc rubs or full annular rubs in rotating machines cause a local heating of the shaft along with a time-varying thermal bow. The time history of machine vibrations, rotor-to-stator contacts and shaft temperature distribution can be simulated by means of accurate mathematical models in which the motion and thermal equations of the system are integrated in the time domain. However, the equivalent bending moments that cause the shaft bow induced by the rubs can be estimated also with model-based identification methods developed in the frequency domain. This strategy does not require to study the complex thermal phenomena that affect the shaft-train since this approach considers only the consequences of the heat generated by the friction forces. Anyhow, these methods allow the severity and the location of the rubs to be identified without requiring time-consuming techniques.

In this paper, the results obtained by the analysis of the rotor-to-stator contacts occurred in a large power unit have been shown and discussed. This investigation have been carried out using a model-based method developed in the frequency domain. This diagnostic strategy provided interesting information about the severity and the development of the fault. This study was very useful to integrate and confirm the results of a root-cause analysis of the fault.

Moreover, the evaluation of the rate of the changes in the amplitude of the shaft bows and of the equivalent bending moments obtained with the proposed diagnostic technique can be used to tune the values of some parameters included in more accurate models in which the motion and thermal equations of the rotating machine are combined with each other and are integrated in the time domain in order to simulate the rub phenomena in detail.

NOMENCLATURE

D: Damping matrix of the fully assembled machine

G: Gyroscopic matrix of the shaft train

K: Stiffness matrix of the fully assembled machine

M: Mass matrix of the fully assembled machine

n: Order number of the harmonic components of the machine vibrations

$\mathbf{F}_n$: Excitation vector associated with the harmonic order n

$\mathbf{H}_n$: Transfer matrix of the machine associated with the order n

$\mathbf{X}_n$: Vibration vector associated with the harmonic order n

$\mathbf{X}_{\text{ex}}$: Vector of the machine experimental vibrations

$\mathbf{X}_m$: Vector of the machine vibrations provided by the simulating model in correspondence with the measurement points

$\mathbf{X}_r$: Vector of the machine vibrations provided by the simulating model in degrees of freedoms that differ from the measurement points

δ: Error between simulated vibrations and experimental data

ε: Residual: relative error between simulated vibrations and experimental data

Ω: Machine angular speed

REFERENCES

[1] A. Muszyńska, *Rotordynamics*, CRC Press, Boca Raton, Fla, USA, 2005.

[2] U. Ehehalt, E. Hahn, and R. Markert, "Experimental validation of various motion patterns at rotor stator contact," in *Proceedings of the 11th International Symposium on Transport Phenomena and Dynamics of Rotating Machinery*, pp. 1–9, Honolulu, Hawaii, USA, February-March 2006, paper 37.

[3] T. Yamamoto and Y. Ishida, *Linear and Nonlinear Rotordynamics: A Modern Treatment with Applications*, John Wiley & Sons, New York, NY, USA, 2001.

[4] R. Liebich and R. Gasch, "Spiral vibrations—modal treatment of a rotor-rub problem based on coupled structural/thermal equations," in *Proceedings of the 6th International Conference on Vibrations in Rotating Machinery (IMechE '96)*, pp. 405–413, London, UK, September 1996.

[5] W. Kellenberger, "Spiral vibrations due to the seal rings in turbogenerators thermally induced interaction between rotor and stator," *Journal of Mechanical Design, Transactions of the ASME*, vol. 102, no. 1, pp. 177–184, 1980.

[6] N. Bachschmid, P. Pennacchi, and A. Vania, "Rotor-to-stator rub causing spiral vibrations—modelling and validation of experimental data on a real rotating machine," in *Proceedings of the 8th International Conference on Vibrations in Rotating Machinery (IMechE '04)*, vol. 2, pp. 671–680, Swansea, UK, September 2004.

[7] N. Bachschmid, P. Pennacchi, and A. Vania, "Identification of multiple faults in rotor systems," *Journal of Sound and Vibration*, vol. 254, no. 2, pp. 327–366, 2002.

[8] A. Vania and P. Pennacchi, "Experimental and theoretical application of fault identification measures of accuracy in rotating machine diagnostics," *Mechanical Systems and Signal Processing*, vol. 18, no. 2, pp. 329–352, 2004.

[9] R. Platz and R. Markert, "Fault models for on-line identification of malfunctions in rotor systems," in *Proceedings of the 4th International Conference on Acoustical and Vibratory Surveillance Methods and Diagnostic Techniques*, pp. 435–446, Compiégne, France, October 2001.

[10] P. Pennacchi, N. Bachschmid, A. Vania, G. A. Zanetta, and L. Gregori, "Use of modal representation for the supporting structure in model-based fault identification of large rotating machinery—part 1: theoretical remarks," *Mechanical Systems and Signal Processing*, vol. 20, no. 3, pp. 662–681, 2006.